Molecular Neurobiology (2019) 56:8336–8344
https://doi.org/10.1007/s12035-019-01671-0

Rostral-Caudal Hippocampal Functional Convergence Is Reduced Across the Alzheimer's Disease Spectrum

Joseph Therriault[1,2,3] · S. Wang[1,2] · S. Mathotaarachchi[1,2] · Tharick A. Pascoal[1,2] · M. Parent[1,2] · T. Beaudry[1,2] · M. Shin[1,2] · Benedet AL[1,2] · M. S. Kang[1,2] · K. P. Ng[1,2] · C. Dansereau[4] · M. T. M. Park[2] · V. Fonov[1,5] · F. Carbonell[5] · E. Zimmer[6] · M. Mallar Chakravarty[2,5] · P. Bellec[4,5] · S. Gauthier[1,4,7] · P. Rosa-Neto[1,4,7] · for the Alzheimer's Disease Neuroimaging Initiative

Received: 19 December 2018 / Accepted: 3 June 2019 / Published online: 22 June 2019

Abstract

Beginning in the early stages of Alzheimer's disease (AD), the hippocampus reduces its functional connections to other cortical regions due to synaptic depletion. However, little is known regarding connectivity abnormalities within the hippocampus. Here, we describe rostral-caudal hippocampal convergence (rcHC), a metric of the overlap between the rostral and caudal hippocampal functional networks, across the clinical spectrum of AD. We predicted a decline in rostral-caudal hippocampal convergence in the early stages of the disease. Using fMRI, we generated resting-state hippocampal functional networks across 56 controls, 48 early MCI (EMCI), 35 late MCI (LMCI), and 31 AD patients from the Alzheimer's Disease Neuroimaging Initiative cohort. For each diagnostic group, we performed a conjunction analysis and compared the rostral and caudal hippocampal network changes using a mixed effects linear model to estimate the convergence and differences between these networks, respectively. The conjunction analysis showed a reduction of rostral-caudal hippocampal convergence strength from early MCI to AD, independent of hippocampal atrophy. Our results demonstrate a parallel between the functional convergence within the hippocampus and disease stage, which is independent of brain atrophy. These findings support the concept that network convergence might contribute as a biomarker for connectivity dysfunction in early stages of AD.

Keywords Alzheimer's disease · Brain network · Functional connectivity · Hippocampus · Mild cognitive impairment

Introduction

Brain network dysfunction in Alzheimer's disease (AD) is associated with the accumulation of tau aggregates in the mesial temporal isocortex [1], which spread to functionally and anatomically connected structures, accompanied by subsequent neurodegeneration [2, 3]. In AD, disrupted patterns of functional connectivity are also present in the hippocampi [4] and their functionally connected structures [5, 6]. In fact, connectivity disruption between the hippocampus and the posterior cingulate cortex can also be observed in mild cognitive impairment (MCI), suggesting that such abnormalities are present at early

Electronic supplementary material The online version of this article (https://doi.org/10.1007/s12035-019-01671-0) contains supplementary material, which is available to authorized users.

✉ Joseph Therriault
joseph.therriault1@gmail.com

[1] McGill University Research Centre for Studies in Aging, Douglas Mental Health University Institute, Montreal, Canada

[2] Douglas Mental Health University Institute, Montreal, Canada

[3] Translational Neuroimaging Laboratory, The McGill University Research Centre for Studies in Aging, Douglas Hospital, McGill University, 6875 La Salle Blvd - FBC room 3149, Montreal, QC H4H 1R3, Canada

[4] Institut universitaire de gériatrie de Montréal, Université de Montréal, Montreal, Canada

[5] McConnell Brain Imaging Centre, Montreal Neurological Institute, Montreal, Canada

[6] Brain Institute of Rio Grande do Sul, Pontifical Catholic University of Rio Grande do Sul (PUCRS), Porto Alegre, RS 90619-900, Brazil

[7] Department of Neurology and Neurosurgery, McGill University, Montreal, Canada

stages of AD [7–10]. However, while hippocampal connectivity with other brain regions has been thoroughly studied, functional connectivity changes within hippocampal areas remain unclear in MCI and AD.

The examination of the Venn diagram–like overlap between two or more independent subnetworks within a given anatomical structure, such as the rostral and caudal networks of the hippocampus, provides an attractive index to test functional convergence of anatomical structures. It is expected that a decline in functional convergence would be observed during the course of neurodegenerative conditions. By employing conjunction analyses, previous research investigating the functional segmentation of brain structures identified areas that converge or share processing components in the amygdala, insula, and cingulate cortex [11, 12]. However, the applications of functional convergence to neurological and psychiatric diseases are poorly understood.

Rostral-caudal hippocampal convergence (rcHC) is of interest in the context of AD due to the early appearance of neurofibrillary tangles in the hippocampus [1], which may disrupt patterns of hippocampal connectivity. While recent research has pointed to a decrease in coherent neuronal activity between the rostral and caudal hippocampus [13, 14], the functional integrity of the hippocampus has received little attention. Crucially, these previous reports failed to differentiate early MCI (EMCI)from late MCI (LMCI), a distinction which allows for a more granular description of the AD spectrum and may identify a distinct clinical stage that may be optimal for disease-modification interventions.

As such, we sought to study the rcHC by probing areas simultaneously connected with both the rostral and caudal hippocampi. Furthermore, we measured the impact of AD stages on the stability of these connections. We hypothesized a progressively declining rcHC functional organization across the pre-dementia stages of AD.

Materials and Methods

Participants

Data used in the preparation of this article were obtained from the Alzheimer's Disease Neuroimaging Initiative (ADNI) database (adni.loni.usc.edu, accessed December 2017). The ADNI was launched in 2003 as a public-private partnership led by principal investigator Michael W. Weiner, MD. The primary goal of ADNI has been to test whether serial MRI, PET, other biological markers, and clinical and neuropsychological assessment can be combined to measure the progression of MCI and early AD.

The ADNI study received approval from the Institutional Review Board of each participating institution. Informed written consent was obtained from all participants in this study.

Participants that are free of memory complaints and have normal memory function, as assessed using a Logical Memory II subscale and the Mini-Mental Score Test (> 24), were characterized as controls. MCI participants were defined as (i) a subjective memory concern as reported by subject, study partner, or clinician; (ii) abnormal memory function documented by scoring within education adjusted ranges; (iii) MMSE score between 24 and 30; (iv) CDR = 0.5 with a memory box score of at least 0.5; and (v) general cognition and functional performance sufficiently preserved such that a diagnosis of AD cannot be made by the site physician at the time of the screening visit. MCI patients were further divided into early and late MCI groups using a Memory Scale Logical Memory II, as specified by ADNI guidelines (Alzheimer's Disease Neuroimaging [15]). AD patients had a Mini-Mental score below 23, presented noticeable behavioral and memory problems, and had amyloid-positive scans, as assessed using a whole-brain (^{18}F)AV-45 PET standard uptake value ratio (SUVR) threshold of 1.26 [16]. Amyloid-negative AD patients were excluded in an effort to obtain a more homogenous group with a similar pathophysiology, given that previous studies demonstrated significant effects of brain amyloid on resting-state networks [17]. The inclusion/exclusion criteria adopted by the ADNI are described in detail at www.adni-info.org (accessed December 2017).

Image Acquisition and Preprocessing

ADNI MRI and rs-fMRI standard acquisition protocols are detailed elsewhere (http://adni.loni.usc.edu/methods; accessed December 2017). The rs-fMRI database was preprocessed using the Neuroimaging Analysis Kit (NIAK) release 0.7.1 [18]. Each rs-fMRI dataset was corrected for inter-slice difference in acquisition time, and the parameters of a rigid-body motion was estimated for each time frame. The median volume of one selected fMRI run for each subject was co-registered with an individual T1 scan using Minctracc [19], which was itself non-linearly transformed to the Montreal Neurological Institute (MNI) standard template [20] using the CIVET pipeline [21] (Fig. 1). The rigid-body transform, fMRI-to-T1 transform, and T1-to-stereotaxic transform were all combined, and the functional volumes were resampled in the MNI space at a 3-mm isotropic resolution. A "scrubbing" method was used to identify volumes with excessive motion (frame displacement greater than 0.5) [22]. The following nuisance parameters were regressed out from the time series at each voxel: slow time drifts (basis of discrete cosines with a 0.01-Hz high-pass and 0.1 low-pass cutoff), average signals in conservative masks of the white matter and the lateral ventricles, and the first principal components (95% energy) of the six rigid-body motion parameters and their squares [23, 24].

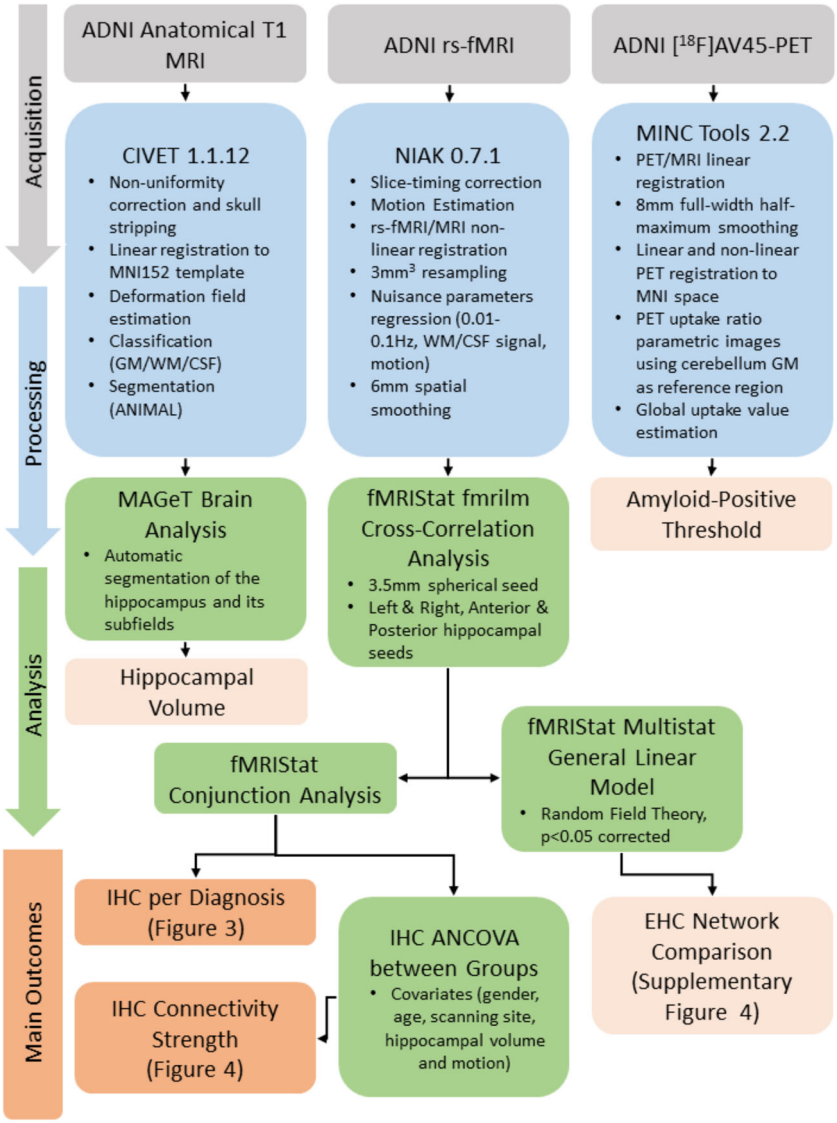

Fig. 1 Summary of imaging analysis steps. Imaging analysis was conducted using four imaging pipelines. CIVET preprocessed structural images, MAGeT performed an automatic segmentation of the hippocampus, NIAK preprocessed rs-fMRI images, and fMRIStat-fmrilm generated the hippocampal connectivity maps. Subsequently, statistical analyses were conducted using fMRIStat-multistat. The primary outcome measures were (1) a conjunction analysis per group and (2) a group comparison of rcHC connectivity strength using analysis of covariance (ANCOVA).

The fMRI volumes were finally spatially smoothed with a 6-mm isotropic Gaussian blurring kernel. A more detailed description of the pipeline can be found on the NIAK website. All images were manually inspected for issues in conversion, co-registration, BOLD signal, and motion using the NIAK protocol.

In order to ensure that hippocampal connectivity decline is not due to declining hippocampal volume, we employed hippocampal volume as a covariate in our analyses. To determine hippocampal volume, T1 MRI images were automatically segmented using the MAGeT Brain algorithm [25, 26]. Five high-resolution atlases of the hippocampus [27] were used as inputs to label a subject of a cohort, automatically generating a template library which is then used for segmentation of individual subjects' MRIs. These methods are described in detail elsewhere [26, 28]. All automated segmentations were manually inspected by an expert rater with over two years of hippocampal segmentation experience. All scans with susceptibility artifacts (i.e., signal dropout) in the medial temporal lobes were excluded. Images that failed co-registration quality assessment by visual inspection were excluded.

Imaging Statistical Analysis

First, we generated functional connectivity maps using the fMRIStat-fmrilm toolbox in MATLAB 2012b [29]. Seeds of 3.5-mm radius spheres were generated for both the left (MNI world coordinates 28, −16, −20) and right (28, −16, −20) anterior, and left (−28, −37, −4) and right (28, −37, −4) posterior hippocampal seeds on the MNI template space in each group. To select the seeds' location, we avoided areas susceptible to hippocampal atrophy and signal dropout, using a probabilistic map of the hippocampi per diagnostic group (Supplementary Fig. 1) and a coefficient of variation map (Supplementary Fig. 2). Finally, an expert rater verified that all seeds were within each

individual's non-linearly transformed T1 MRI hippocampi. The seed selection process is illustrated in Fig. 2.

Subsequently, we concatenated multiple fMRI runs to generate one connectivity map for each subject with a fixed effects general linear model, using the fMRIStat toolbox. To measure rcHC, we performed a conjunction analysis between the rostral and caudal seed in each diagnostic group to highlight the regions simultaneously functionally connected with the rostral and caudal seed (Fig. 3) [30]. In the present analysis, performing a conjunction analysis provides a measure of integration between the rostral and caudal hippocampal systems across disease stages. Conjunction, the joint refutation of multiple null hypotheses [31], is stringent in nature as it requires the co-occurrence of functional significance in independent brain images and has been previously used to characterize patterns of activation in other brain structures [32]. Performing a conjunction analysis provides a measure of integration between the anterior and posterior hippocampal systems, providing information about rcHC changes within a disease. Because the present study employed only two statistic maps in every conjunction analysis (one for the rostral and caudal hippocampal seeds), this method is valid for determining the conjunction of the two separate effects [33].

Then, the overlapping areas within the hippocampi in controls served as a mask, which was applied to every individual connectivity map. The average z-values under the mask were calculated, corresponding to the rcHC network strength, and served as input for the analysis of covariance (ANCOVA) model to compute group differences. Sex, age, scanning site, motion, and hippocampal volume served as covariates to determine group differences. The average and 95% confidence interval are depicted in Fig. 4. To determine if there is added value of rcHC over hippocampal volume as a biomarker of disease severity, we conducted an independent sample t test comparing the hippocampal volumes of early MCI (EMCI) and late MCI (LMCI).

To validate our dataset with previous findings, we assessed the patterns of functional connectivity between the hippocampus and other brain structures and generated group-level t-statistical parametric maps of correlation coefficients using a mixed effects model (connectivity maps using multistat in fMRIStat toolbox), with sex, age, scanning site, motion, and hippocampal volume as covariates. We masked these extra-hippocampal connectivity parametric maps with the average connectivity maps from controls, thresholded at $p \leq 0.05$ to discard regions uncorrelated with the seed points, and corrected for multiple comparisons using a Random Field Theory (RFT) statistical significance level of $p \leq 0.05$ [34, 35]. Differences in extra-hippocampal connectivity between controls and patient groups are presented in Fig. 5. Laterality differences in extra-hippocampal connectivity are presented in Supplementary Fig. 4. Figures were projected on a volume or surface space and generated using MINC Register, Display, and NeuroVault [36].

Data Availability Data used in preparation of this article were obtained from the Alzheimer's Disease Neuroimaging Initiative (ADNI) database (adni.loni.usc.edu). As such, the investigators within the ADNI contributed to the design and implementation of ADNI and/or provided data but did not participate in analysis or writing of this report. A complete listing of ADNI investigators can be found at: http://adni.loni.usc.edu/wp-content/uploads/how_to_apply/ADNI_Acknowledgement_List.pdf

Results

Demographic Differences

Out of 194 participants, six AD patients were amyloid-negative and therefore excluded. An additional 18 subjects were excluded during quality control because of poor acquisition (ex. signal dropout), or co-registration failures.

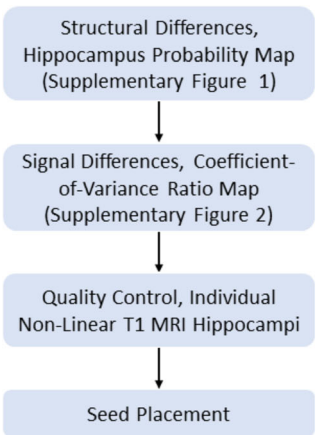

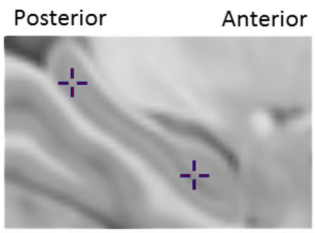

Seed Location	World Voxels, MNI152 Template (x,y,z)
Left Anterior Hippocampus	(-28,-16,-20)
Right Anterior Hippocampus	(28,-16,-20)
Left Posterior Hippocampus	(-28,-37,-4)
Right Posterior Hippocampus	(28,-37,-4)

Fig. 2 Seed selection process. The seed selection process took into account the structural differences of the hippocampus, as well as the resting-state fMRI signal strength. The seed points are placed in areas (1) with low susceptibility to atrophy and signal drop-out and (2) within the range of the hippocampus across all individuals after non-linear co-registration

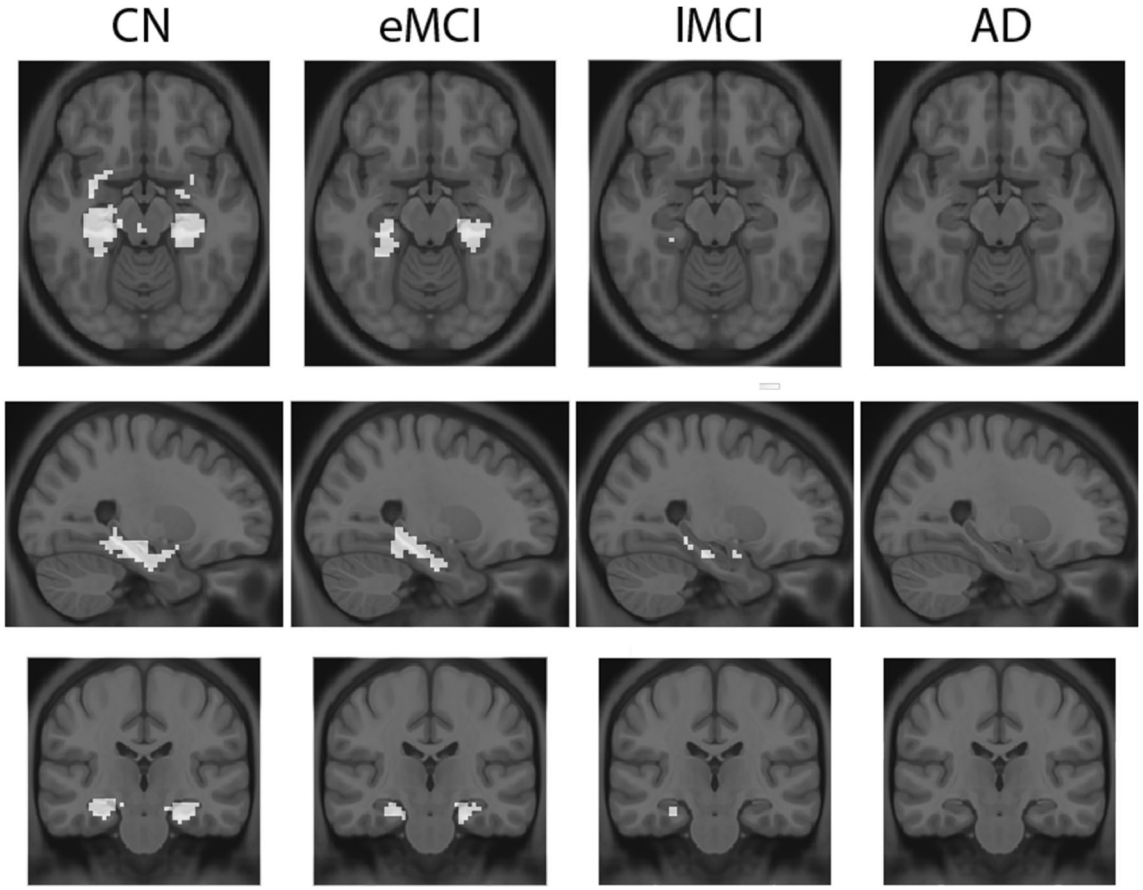

Fig. 3 Reduced rcHC in patients with more advanced disease. rcHC, as defined by the conjunction analysis between the rostral and caudal hippocampal networks, is reduced in patients with more advanced disease (highlighted in white). The figure is a result of the collapses across all subjects within a group

No differences in age, sex, and education were observed. Furthermore, no differences in image frame displacement were observed between disease groups. MMSE scores ($p \leq 0.001$), ApoE4 genetic ($p \leq 0.001$), and amyloid status ($p \leq 0.001$) were significantly different in AD (Table 1).

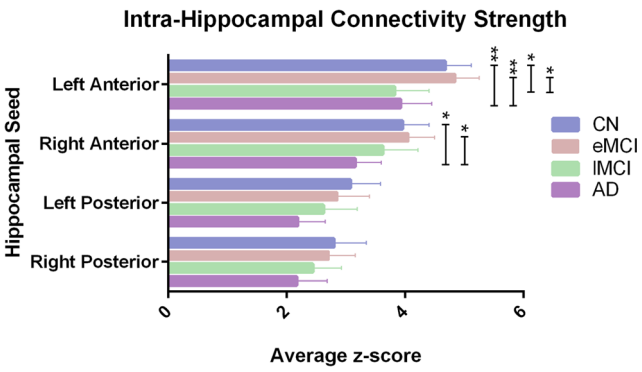

Fig. 4 Individual rcHC connectivity strength by seed and diagnosis group. The error bars show the 95% confidence interval. While both the left and right anterior rcHC showed declines with disease severity, the posterior seeds did not. *$p \leq 0.05$, **$p \leq 0.01$

The Intra-Hippocampal Network Conjunction Diminishes with Disease Severity

The conjunction analysis showed significant overlap in healthy controls between the rostral and caudal hippocampal networks. In patients with a more severe disease, we observed a bilateral decrease of the overlap in between the hippocampal networks (Fig. 3). These results are independent of declining hippocampal volume across disease states and of in-scanner head motion as both were employed as covariates in the linear model. No significant difference in hippocampal volume was observed between EMCI (4564 ± 547) and LMCI (4786 ± 603) ($p = 0.0841$).

RcHC Strength Decrease Is Driven by Changes in the Anterior Hippocampal Network

The left anterior rcHC strength was decreased in patients with more severe disease (EMCI vs controls, $p = 1$; LMCI vs controls, $p = 0.037$; AD vs controls, $p = 0.007$), whereas the left posterior hippocampus remained the same (EMCI vs controls, $p = 1$; LMCI vs controls, $p = 0.60$; AD vs controls, $p = 0.11$) (Fig. 4). The decline was also present with the right anterior

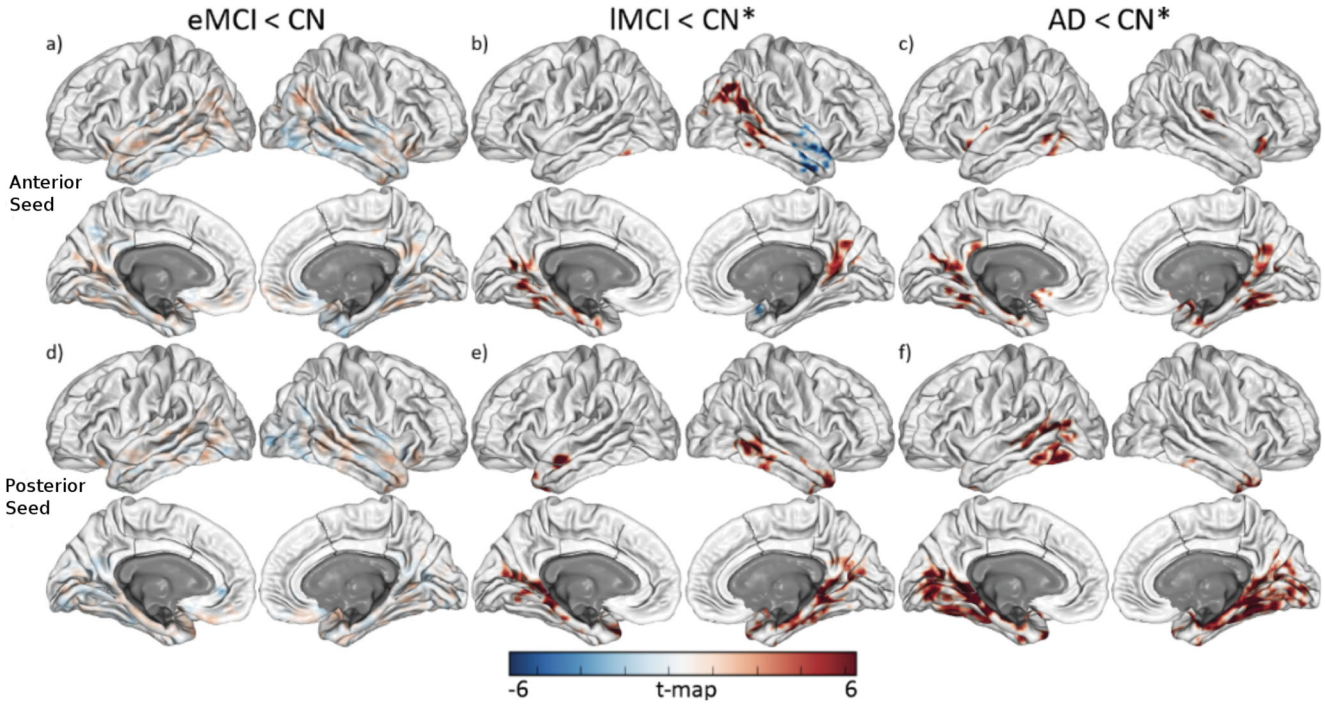

Fig. 5 Extra-hippocampal connectivity differences between controls and patient diagnostic groups. Positive *t* values indicate a reduction in the connectivity in the disease state vs controls. Whereas EMCI showed no differences, both LMCI and AD suffered connectivity decreases between the anterior hippocampus and the parahippocampal gyrus, the PCC, and the inferior parietal cortex. In addition, LMCI and AD also showed decreases in the connectivity between the posterior hippocampus and the middle temporal gyrus, the fusiform gyrus, and the occipital lobe. No significant connectivity increases in disease states were observed. Connectivity increases *RFT-corrected (LMCI and AD, corrected threshold $p \leq 0.05$), with minimum cluster size = 238 mm^3 and supra threshold = 3.1893 for the controls vs AD contrast

seed (EMCI vs controls, $p = 0.99$; LMCI vs controls, $p = 0.52$; AD vs controls, $p = 0.046$), but not the right posterior hippocampus (EMCI vs controls, $p = 0.99$; LMCI vs controls, $p = 0.59$; AD vs controls, $p = 0.27$).

Reductions in Whole-Brain Extra-Hippocampal Connectivity in LMCI and AD Compared with Controls

No significant differences were observed between EMCI and controls after multiple comparison correction. In contrast, LMCI patients, when compared with controls, showed widespread functional disruptions between both the anterior and posterior hippocampi and the whole brain. AD patients exhibited similar disconnection patterns to LMCI, but with larger and more extended regions (Fig. 5).

Discussion

In summary, we characterized rcHC as the overlap between the rostral and caudal functional networks of the hippocampus. We expanded on previous investigations of functional

Table 1 Group demographics

	Controls	EMCI	LMCI	AD
N	56	48	35	31
Age (years)	75 ± 7	72 ± 7	73 ± 8	73 ± 7
Sex (% male)	55.4%	54.2%	40.0%	58.1%
Handedness (% right-handed)	87.5%	98.0%	94.3%	93.5%
Education (years)	17 ± 2	16 ± 3	17 ± 2	16 ± 3
MMSE (/30)	29 ± 2	28 ± 2	28 ± 2	23 ± 3***
ApoE4 (% positive)	28.6%	47.9%	37.1%	58.1%***
Hippocampus volume (mm^3)	4871 ± 615	4564 ± 547	4786 ± 603	4238 ± 655***
Frame displacement (mm)	0.3 ± 0.1	0.3 ± 0.2	0.3 ± 0.1	0.3 ± 0.1

Mean ± standard deviation. *$p \leq 0.05$, **$p \leq 0.01$, ***$p \leq 0.001$. Significance is calculated as compared with controls

connectivity in AD by employing a conjunction analysis, which provides a measure of convergence between the rostral and caudal hippocampal systems, and permits us to follow the rcHC changes within a disease. We found that rcHC reductions were apparent in LMCI and AD, were driven by a declining anterior network bilaterally, and were independent of hippocampal volume. Furthermore, rcHC in the left anterior hippocampal seed proved more sensitive than hippocampal volume in distinguishing EMCI from LMCI. Finally, we validated our dataset by generating connectivity maps between the hippocampus and the rest of the brain and observing declines in LMCI and AD, in agreement with previous findings [4, 37]. While we did not observe changes between cognitively normal controls and EMCI, this could be because the present analyses were corrected for hippocampal volume in contrast to previous studies reporting differences between cognitively normal and EMCI subjects [38].

Disrupted patterns of connectivity within and outside of the hippocampus were simultaneously observed in LMCI but not in earlier states, suggesting that AD pathophysiology affects a hippocampal hub connected to both internal and external regions. Combined with the dissociation between the anterior and posterior hippocampus, our results suggest that such a hub resides in the anterior section of the hippocampus. In addition, no increases in rcHC were observed with increasing disease severity, suggesting that rcHC may be a useful functional biomarker of AD because it does not confound the compensatory neural activity frequently observed in other fMRI biomarkers [39, 40]. Because rcHC but not hippocampal volume was different between EMCI and LMCI, our results suggest that changes in functional convergence may prove to be a sensitive biomarker of disease severity along the AD spectrum.

The functional role of the hippocampus varies across its longitudinal axis; specifically, the anterior hippocampus contributes to emotional reactions and the posterior hippocampus to cognitive functions [41, 42]. As such, our results—the disruption of the anterior system and preservation of the posterior one—fit with early AD neuropsychiatric symptoms of apathy and mood disorders [43–45]. Furthermore, the absence of a conjunction between the anterior and the posterior hippocampi in LMCI indicates hippocampal dysfunction in individuals close to converting to AD. As these functional connections are a substrate of the BOLD signal, our findings may be related to synaptic activity changes [46]. Indeed, previous histological investigations suggest the loss of hippocampal cells and the deletion of synapses during the course of AD. In particular, the dentate gyrus exhibits reduced number of synapses in the outer molecular layer in early AD; CA1 has lower synaptic gene expression and neuronal count in MCI; and CA3 neuronal density is decreased in AD [47–51]. In addition, these synaptic density changes are highly correlated with cognitive impairment [52]. Since a significant part of the hippocampal formation's intra-circuitry is unidirectional, from the dentate gyrus to the subiculum, any disruption along that path will likely contribute to decline in rcHC [53].

Some methodological limitations of our study make replication of these results desirable. Firstly, the ADNI dataset control cohort tends to be more educated with a higher MMSE score and have a higher representation of participants with a family history of AD. Secondly, despite correcting for structural changes using a non-linear co-registration and including the volume of the hippocampus as covariate across our analyses, it remains possible that structural differences such as hippocampal shape [54] impacted the present results. Furthermore, because amyloid positivity was not an inclusion criteria for the control and MCI subjects, we cannot conclude that these results are representative of the entire Alzheimer's disease spectrum, as some individuals may not have Alzheimer's pathology. Finally, given the cross-sectional nature of the present study, our results cannot infer a predictive value of the hippocampal connectivity in the progression towards AD.

In conclusion, we observed a decline in hippocampal functional network convergence in EMCI, LMCI, and AD. Furthermore, the anterior hippocampal network is disrupted in LMCI and AD and loses its synergy in patients with more advanced disease. Our study warrants the segregation of hippocampal subfields across its longitudinal axis when conducting imaging studies. Finally, our results support a framework for the investigation of functional convergence as a biomarker of neurological and psychiatric disorders.

Funding This work was supported by the Canadian Institutes of Health Research (CIHR) (MOP-11-51-31); the Alan Tiffin Foundation; the Alzheimer's Association (NIRG-08-92090); and the Fonds de recherche du Québec—Santé (chercheur boursier); the CAPES Foundation (0327/13-1), and a fellowship from the Stop-AD Centre, provided by McGill University and the Douglas Hospital Research Centre Institutional Funding. Data collection and sharing for this project was funded by the Alzheimer's Disease Neuroimaging Initiative (ADNI) (National Institutes of Health Grant U01 AG024904) and DOD ADNI (Department of Defense award number W81XWH-12-2-0012). ADNI is funded by the National Institute on Aging, the National Institute of Biomedical Imaging and Bioengineering, and through generous contributions from the following: Alzheimer's Association; Alzheimer's Drug Discovery Foundation; Araclon Biotech; BioClinica, Inc.; Biogen Idec Inc.; Bristol-Myers Squibb Company; Eisai Inc.; Elan Pharmaceuticals, Inc.; Eli Lilly and Company; EuroImmun; F. Hoffmann-La Roche Ltd., and its affiliated company Genentech, Inc.; Fujirebio; GE Healthcare; IXICO Ltd.; Janssen Alzheimer Immunotherapy Research & Development, LLC.; Johnson & Johnson Pharmaceutical Research & Development LLC.; Medpace, Inc.; Merck & Co., Inc.; Meso Scale Diagnostics, LLC.; NeuroRx Research; Neurotrack Technologies; Novartis Pharmaceuticals Corporation; Pfizer Inc.; Piramal Imaging; Servier; Synarc Inc.; and Takeda Pharmaceutical Company. The Canadian Institutes of Health Research is providing funds to support ADNI clinical sites in Canada. Private sector contributions are facilitated by the Foundation for the National Institutes of Health (www.fnih.org). The grantee organization is the Northern California Institute for Research and Education, and the study is coordinated by the Alzheimer's Disease Cooperative Study at the University of California, San Diego. ADNI data are disseminated by the Laboratory for Neuro Imaging at the University of Southern California.

Compliance with Ethical Standards

In this section, we outline our manuscript's compliance with all relevant ethical standards.

Conflict of Interest Therriault J, Wang S, Mathotaarachchi S, Pascoal TA, Parent M, Beaudry T, Shin M, Benedet AL, Kang MS, Ng KP, Dansereau C, Park MTM, Fonov V, Carbonell F, Zimmer E, Chakravarty M, Bellec P, and Rosa-Neto P have no conflicts of interest to disclose. S. Gauthier has received honoraria for serving on the scientific advisory boards of Alzheon, Axovant, Lilly, Lundbeck, Novartis, Schwabe, and TauRx and on the Data Safety Monitoring Board of a study sponsored by Eisai and studies run by the Alzheimer's Disease Cooperative Study and by the Alzheimer's Therapeutic Research Institute.

Ethical Approval All procedures performed in studies involving human participants were in accordance with the ethical standards of the institutional and/or national research committee and with the 1964 Helsinki declaration and its later amendments or comparable ethical standards.

Informed Consent The ADNI study was approved by the Institutional Review Boards of all of the participating institutions. Informed written consent was obtained from all participants in the study.

References

1. Braak H, Braak E (1991) Neuropathological stageing of Alzheimer-related changes. Acta Neuropathologica 82:239–259
2. Chiotis K, Leuzy A, Almkvist O, et al (2017) Longitudinal changes of tau PET imaging in relation to hypometabolism in prodromal and Alzheimer's disease dementia. Mol Psychiatry 1–8. doi: https://doi.org/10.1038/mp.2017.108
3. Seeley WW, Crawford RK, Zhou J, Miller BL, Greicius MD (2009) Neurodegenerative diseases target large-scale human brain networks. Neuron 62:42–52. https://doi.org/10.1016/j.neuron.2009.03.024
4. Allen G, Barnard H, Mccoll R et al (2007) Reduced hippocampal functional connectivity in Alzheimer disease. Arch Neurol 64:1482–1487
5. Badhwar A, Tam A, Dansereau C et al (2017) Resting-state network dysfunction in Alzheimer's disease: a systematic review and meta-analysis. Alzheimer's & Dementia: Diagnosis, Assessment & Disease Monitoring 8:73–85
6. Greicius MD, Srivastava G, Reiss AL, Menon V (2004) Default-mode network activity distinguishes Alzheimer's disease from healthy aging: evidence from functional MRI. Proc Natl Acad Sci 101:4637–4642
7. Bai F, Watson DR, Yu H, Shi Y, Yuan Y, Zhang Z (2009) Abnormal resting-state functional connectivity of posterior cingulate cortex in amnestic type mild cognitive impairment. Brain Res 1302:167–174. https://doi.org/10.1016/j.brainres.2009.09.028
8. Sorg C, Riedl V (2007) Selective changes of resting-state networks in individuals at risk for Alzheimer's disease. Proceedings of the National Academy of Sciences 104:18760–18765
9. Wu L, Soder RB, Schoemaker D, Carbonnell F, Sziklas V, Rowley J, Mohades S, Fonov V et al (2014) Resting state executive control network adaptations in amnestic mild cognitive impairment. J Alzheimers Dis 40:1–12. https://doi.org/10.3233/JAD-131574
10. Zhou Y, Dougherty JH, Hubner KF et al (2008) Abnormal connectivity in the posterior cingulate and hippocampus in early Alzheimer's disease and mild cognitive impairment. Alzheimers Dement 4:265–270. https://doi.org/10.1016/j.jalz.2008.04.006
11. Roy AK, Shehzad Z, Margulies DS, Kelly AMC, Uddin LQ, Gotimer K, Biswal BB, Castellanos FX et al (2009) Functional connectivity of the human amygdala using resting state fMRI. NeuroImage 45:614–626. https://doi.org/10.1016/j.neuroimage.2008.11.030
12. Taylor KS, Seminowicz DA, Davis KD (2009) Two systems of resting state connectivity between the insula and cingulate cortex. Hum Brain Mapp 30:2731–2745. https://doi.org/10.1002/hbm.20705
13. Pasquini L, Scherr M, Tahmasian M et al (2014) Link between hippocampus' raised local and eased global intrinsic connectivity in AD. Alzheimers Dement 11:475–484
14. Zarei M, Beckmann CF, Binnewijzend MAA et al (2013) Functional segmentation of the hippocampus in the healthy human brain and in Alzheimer's disease. NeuroImage 66:28–35. https://doi.org/10.1016/j.neuroimage.2012.10.071
15. Alzheimer's Disease Neuroimaging Initiative (2005) ADNI2 procedures manual
16. Biomedical Research Forum LLC (2015) When there's no amyloid, it's not Alzheimer's. AlzForum
17. Hedden T, Van Dijk KRA, Becker JA et al (2009) Disruption of functional connectivity in clinically normal older adults harboring amyloid burden. J Neurosci 29:12686–12694. https://doi.org/10.1523/JNEUROSCI.3189-09.2009
18. Bellec P, Carbonell FM, Perlbarg V, et al (2011) A neuroimaging analysis kit for Matlab and Octave. In: Proceedings of the 17th international conference on functional mapping of the human brain pp. 2735–46
19. Collins DL, Evans AC (1997) Animal: validation and applications of nonlinear registration-based segmentation. Int J Pattern Recognit Artif Intell 11:1271–1294. https://doi.org/10.1142/S0218001497000597
20. Fonov V, Evans AC, Botteron K, Almli CR, McKinstry R, Collins DL, Brain Development Cooperative Group (2011) Unbiased average age-appropriate atlases for pediatric studies. NeuroImage 54:313–327. https://doi.org/10.1016/j.neuroimage.2010.07.033
21. Zijdenbos AP, Forghani R, Evans AC (2002) Automatic "pipeline" analysis of 3-D MRI data for clinical trials: application to multiple sclerosis. IEEE Trans Med Imaging 21:1280–1291. https://doi.org/10.1109/TMI.2002.806283
22. Power JD, Barnes KA, Snyder AZ, Schlaggar BL, Petersen SE (2012) Spurious but systematic correlations in functional connectivity MRI networks arise from subject motion. Neuroimage 59:2142–2154. https://doi.org/10.1016/j.neuroimage.2011.10.018
23. Giove F, Gili T, Iacovella V, Macaluso E, Maraviglia B (2009) Images-based suppression of unwanted global signals in resting-state functional connectivity studies. Magn Reson Imaging 27:1058–1064. https://doi.org/10.1016/j.mri.2009.06.004
24. Lund TE, Madsen KH, Sidaros K, Luo WL, Nichols TE (2006) Non-white noise in fMRI: does modelling have an impact? NeuroImage 29:54–66. https://doi.org/10.1016/j.neuroimage.2005.07.005
25. Chakravarty MM, Steadman P, Eede MC et al (2013) Performing label-fusion-based segmentation using multiple automatically generated templates. Hum Brain Mapp 34:2635–2654
26. Pipitone J, Park MTM, Winterburn J, Lett TA, Lerch JP, Pruessner JC, Lepage M, Voineskos AN et al (2014) Multi-atlas segmentation of the whole hippocampus and subfields using multiple automatically generated templates. Neuroimage 101:494–512
27. Winterburn JL, Pruessner JC, Chavez S, Schira MM, Lobaugh NJ, Voineskos AN, Chakravarty MM (2013) A novel in vivo atlas of human hippocampal subfields using high-resolution 3T magnetic resonance imaging. Neuroimage 74:254–265

28. Treadway MT, Waskom ML, Dillon DG, Holmes AJ, Park MTM, Chakravarty MM, Dutra SJ, Polli FE et al (2015) Illness progression, recent stress, and morphometry of hippocampal subfields and medial prefrontal cortex in major depression. Biol Psychiatry 77: 285–294
29. Worsley KJ, Liao CH, Aston J, Petre V, Duncan GH, Morales F, Evans AC (2002) A general statistical analysis for fMRI data. NeuroImage 15:1–15. https://doi.org/10.1006/nimg.2001.0933
30. Worsley K, Friston K (2000) A test for a conjunction. Statistics and Probability Letters 47:135–140. https://doi.org/10.1016/S0167-7152(99)00149-2
31. Friston KJ, Holmes AP, Price CJ, et al (1999) Multisubject fMRI studies and conjunction analyses. NeuroImage 10:385–396
32. Persson J, Nyberg L (2000) Conjunction analysis of cortical activations common to encoding and retrieval. Microsc Res Tech 51:39–44
33. Friston KJ, Penny WD, Glaser DE (2005) Conjunction revisited. doi: https://doi.org/10.1016/j.neuroimage.2005.01.013
34. Friston KJ, Worsley KJ, Frackowiak RSJ et al (1993) Assessing the significance of focal activations using their spatial extent. Hum Brain Mapp 1:210–220
35. Worsley KJ, Cao J, Paus T, Petrides M, Evans AC (1998) Applications of random field theory to functional connectivity. Hum Brain Mapp 6:364–367
36. Gorgolewski KJ, Yarkoni T, Ghosh SS, et al (2013) NeuroVault.org: a web database for sharing statistical parametric maps. In: 19th Annual Meeting of the Organization for Human Brain Mapping
37. Jones DT, Knopman DS, Gunter JL, Graff-Radford J, Vemuri P, Boeve BF, Petersen RC, Weiner MW et al (2016) Cascading network failure across the Alzheimer's disease spectrum. Brain 139: 547–562. https://doi.org/10.1093/brain/awv338
38. Lee E-S, Yoo K, Lee Y-B, Chung J, Lim JE, Yoon B, Jeong Y, Alzheimer's Disease Neuroimaging Initiative (2016) Default mode network functional connectivity in early and late mild cognitive impairment. Alzheimer Dis Assoc Disord 30:289–296. https://doi.org/10.1097/wad.0000000000000143
39. Bondi MW, Houston WS, Eyler LT, Brown GG (2005) fMRI evidence of compensatory mechanisms in older adults at genetic risk for Alzheimer disease. Neurology 64:501–508. https://doi.org/10.1212/01.WNL.0000150885.00929.7E
40. Huijbers W, Mormino EC, Schultz AP, Wigman S, Ward AM, Larvie M, Amariglio RE, Marshall GA et al (2015) Amyloid-β deposition in mild cognitive impairment is associated with increased hippocampal activity, atrophy and clinical progression. Brain 138:1023–1035. https://doi.org/10.1093/brain/awv007
41. Fanselow MS, Dong H-W (2010) Are the dorsal and ventral hippocampus functionally distinct structures? Neuron 65:7–19. https://doi.org/10.1016/j.neuron.2009.11.031
42. Strange BA, Witter MP, Lein ES, Moser EI (2014) Functional organization of the hippocampal longitudinal axis. Nat Rev Neurosci 15:655–669. https://doi.org/10.1038/nrn3785
43. Hamann S, Monarch ES, Goldstein FC (2002) Impaired fear conditioning in Alzheimer's disease. Neuropsychologia 40:1187–1195. https://doi.org/10.1016/S0028-3932(01)00223-8
44. Landes AM, Sperry SD, Strauss ME, Geldmacher DS (2001) Apathy in Alzheimer's disease. J Am Geriatr Soc 49:1700–1707
45. Therriault J, Ng KP, Pascoal TA, Mathotaarachchi S, Kang MS, Struyfs H, Shin M, Benedet AL et al (2018) Anosognosia predicts default mode network hypometabolism and clinical progression to dementia. Neurology 90:e932–e939. https://doi.org/10.1212/WNL.0000000000005120
46. Viswanathan A, Freeman RD (2007) Neurometabolic coupling in cerebral cortex reflects synaptic more than spiking activity. Nature Neuroscience 10:1308–1312
47. Counts SE, Alldred MJ, Che S, Ginsberg SD, Mufson EJ (2014) Synaptic gene dysregulation within hippocampal CA1 pyramidal neurons in mild cognitive impairment. Neuropharmacology 79: 172–179
48. Padurariu M, Ciobica A, Mavroudis I et al (2012) Hippocampal neuronal loss in the Ca1 and Ca3 areas of Alzheimer's disease patients. Psychiatr Danub 24:152–158
49. Scheff SW, Price DA, Schmitt FA, Mufson EJ (2006) Hippocampal synaptic loss in early Alzheimer's disease and mild cognitive impairment. Neurobiol Aging 27:1372–1384
50. West MJ, Coleman PD, Flood DG, Troncoso JC (1994) Differences in the pattern of hippocampal neuronal loss in normal aging and Alzheimer's-disease. Lance 344:769–772. https://doi.org/10.1016/S0140-6736(94)92338-8
51. West MJ, Kawas CH, Martin LJ, Troncoso JC (2000) The CA1 region of the human hippocampus is a hot spot in Alzheimer's disease. Annals of the New York Academy of Sciences 908:255–259
52. Scheff SW, Price DA (2006) Alzheimer's disease-related alterations in synaptic density: neocortex and hippocampus. J Alzheimers Dis 9:101–115
53. Mai JK, Paxinos G (2011) The human nervous system. Academic press
54. Voineskos AN, Winterburn JL, Felsky D, Pipitone J, Rajji TK, Mulsant BH, Chakravarty MM (2015) Hippocampal (subfield) volume and shape in relation to cognitive performance across the adult lifespan. Hum Brain Mapp 36:3020–3037. https://doi.org/10.1002/hbm.22825